

# RSC Advances



This is an *Accepted Manuscript*, which has been through the Royal Society of Chemistry peer review process and has been accepted for publication.

*Accepted Manuscripts* are published online shortly after acceptance, before technical editing, formatting and proof reading. Using this free service, authors can make their results available to the community, in citable form, before we publish the edited article. This *Accepted Manuscript* will be replaced by the edited, formatted and paginated article as soon as this is available.

You can find more information about *Accepted Manuscripts* in the [Information for Authors](#).

Please note that technical editing may introduce minor changes to the text and/or graphics, which may alter content. The journal's standard [Terms & Conditions](#) and the [Ethical guidelines](#) still apply. In no event shall the Royal Society of Chemistry be held responsible for any errors or omissions in this *Accepted Manuscript* or any consequences arising from the use of any information it contains.



Journal Name

COMMUNICATION

## Plasma Protein Corona Reduces the Haemolytic Activity of the Graphene Oxide Nano and Micro Flakes

M. Papi<sup>a\*</sup>, M.C. Lauriola<sup>a</sup>, V. Palmieri<sup>a</sup>, G. Ciasca<sup>a</sup>, G. Maulucci<sup>a</sup> and M. De Spirito<sup>a</sup>Received 00th January 20xx,  
Accepted 00th January 20xx

DOI: 10.1039/x0xx00000x

www.rsc.org/

The intensive research on the bio-applications of graphene and derivatives are leading to many technological applications. Graphene Oxide (GO), for its unique 2-D structure and its physical/chemical properties, has attracted increasing interest over the last years in the fields of drug/gene delivery, biological imaging and antibacterial treatments. Together with these great potential on the biomedical applications, several aspects about graphene toxicity mechanisms including oxidative stress, cutting off intracellular metabolic routes and cell membrane rupture must be carefully evaluated. In this work we demonstrate that the GO flakes, able to disrupt the erythrocytes plasma membrane, greatly reduce their hemolytic activity after interacting with plasma proteins.

### Introduction

Graphene, as a graphitic nanomaterial, is a flat monolayer made of sp<sup>2</sup>-bonded carbon atoms tightly packed in a honeycomb lattice. As a result of these fascinating properties graphene offers some important advantages for biotechnological applications, especially in the areas of bioelectronics, biosensors and medicine<sup>1,2</sup>. However, the merging of graphene and biotechnology is in its infancy, with many challenges remaining. One of the most important aspects still open is the graphene toxicology and therefore its potential risk, in light of the increased use and likelihood of exposure<sup>3-5</sup>. Graphene flakes physicochemical properties must be examined in detail to create the correct design rules and to begin interpreting any results due to graphene-induced toxicity. Because this material is relatively new and the specific properties that influence cellular toxicity are still not fully understood, a thorough characterization is essential.

Graphene oxide (GO), the disordered analogue of crystalline graphene, is highly oxidized with large numbers of residual epoxides, hydroxides and carboxylic acid groups on its surface. GO allows higher interaction with a wide range of organic and inorganic materials because of its oxygen-containing functional groups<sup>6</sup>. Various biomedical applications were proposed based on the physical and chemical properties of GO such as drug and gene delivery. However nanomaterials for delivery in the bloodstream have to be studied in light of the interaction and lysis of the erythrocytes. Recently a concentration-dependent GO toxicity in human erythrocytes has been reported<sup>7</sup>. Erythrocytes toxicity has been assessed by measuring hemolysis, i.e. the release of hemoglobin upon cell lysis, under various exposure conditions. Involvement of the reactive oxygen species (ROS) generated by GO and the direct contact interaction of extremely sharp edges of graphene nanowalls with cells membranes are reputed the main mechanisms involved in GO flakes cytotoxicity<sup>4,7-10</sup>. It has been also observed that coating GO with chitosan or amine nearly eliminated its hemolytic activity demonstrating that particle size, particulate state, oxygen content and surface charge of graphene have a strong impact on biological/toxicological responses on red blood cells<sup>7,11,12</sup>.

In this work we investigate the cytotoxicity of GO flakes in human erythrocytes taking into account that, after the injection in the bloodstream, they are exposed to a wide range of plasma proteins. This phenomenon significantly affects the fate of GO in biological systems including its cellular uptake and consequent toxic responses. GO flakes pristine surfaces are immediately covered by biomolecules (proteins, lipids, enzymes) upon their entrance into a biological medium. These coated surfaces confer a new "biological identity" to the nanosystem consisting of hydrophilicity/hydrophobicity, surface charges and topography<sup>13</sup>. This new identity determines the biological responses at the cellular and tissue level. Because of their high specific surface area, the carbon family of nanomaterials, including graphene, possesses potentially larger protein adsorption capacities than other nano-objects<sup>9,14,15</sup>.

<sup>a</sup> Istituto di Fisica, Università Cattolica del sacro Cuore, Largo F. Vito 1, 00168 Roma, Italy. E-mail: m.papi@m.unicatt.it.

† Footnotes relating to the title and/or authors should appear here. Electronic Supplementary Information (ESI) available: [details of any supplementary information available should be included here]. See DOI: 10.1039/x0xx00000x

## Experimental

To obtain different GO flakes sizes a GO solution at 200  $\mu\text{g}/\text{ml}$  (Graphenea) was sonicated for 1, 5, 10, 20 minutes with a probe-sonicator at 50 W (VC50 Sonics and Materials UK). Sonicated solutions were centrifuged at 16000 g for 5 minutes and pellets were resuspended in saline buffer. To induce the formation of protein corona on the GO flakes (GO+PC), GO sonicated samples were incubated in ice bath (1 hour), and subsequently at 37°C (1 hour) with 10  $\mu\text{l}$  of plasma from fresh Lilio Eparin stabilized human whole blood. Human whole blood was obtained by venepuncture of ten healthy volunteers at the Policlinico Gemelli of Rome in accordance with the institutional bioethics code. Formation of a protein corona on the GO-flakes was assessed by Transmission Electron Microscopy (TEM), Dynamic Light Scattering (DLS) and  $\zeta$ -potential. DLS and  $\zeta$ -potential of samples were performed with Zetasizer Nano ZS (Malvern, Herrenberg, Germany). The  $\zeta$ -potential was calculated from the electrophoretic mobility by means of the Henry correction to Smoluchowski's equation<sup>16</sup> and the size distribution was calculated by using the regularized Laplace inversion of the light scattering intensity autocorrelation function<sup>17</sup>. TEM (Zeiss Libra 120) was used to visualize GO and GO+PC structures stained with uranyl acetate as described elsewhere<sup>18</sup>. Atomic Force Microscopy (AFM) (NanoWizard II, JPK, Germany) was used to measure the thickness of GO and GO+PC samples.

Haemolytic effects were investigated by spectrophotometric measurements and confocal imaging. Briefly, 1 ml of whole blood was diluted and centrifuged at 500 g for 5 minutes to isolate Red Blood Cells (RBC) from serum. To test the haemolytic activity of both GO and GO+PC, 0.2 ml of diluted RBCs solution was added to 0.8 ml of GO and GO+PC solutions and let interact at 37°C for 3 hours. RBC in double distilled water (ddH<sub>2</sub>O) and RBC in saline buffer were used as positive and negative control, respectively. After incubation the samples were centrifuged at 4000 g for 5 min and the supernatant recovered. The haemoglobin absorbance in the supernatant was measured at 540 nm and the Haemolysis was calculated as follows:

$$\text{Haemolysis}(\%) = \left( \frac{\text{sample}_{540\text{nm}} - \text{negControl}_{540\text{nm}}}{\text{posControl}_{540\text{nm}} - \text{negControl}_{540\text{nm}}} \right) \quad (1)$$

Where  $\text{sample}_{540\text{nm}}$ ,  $\text{negControl}_{540\text{nm}}$  and  $\text{posControl}_{540\text{nm}}$  are the absorbance measured for the sample, the positive and the negative control respectively<sup>7</sup>.

Hematoxylin–eosin stained erythrocytes were imaged with a CARV II spinning-disk microscope (Crisel Instruments, Rome, Italy).

## Results and discussion

In Fig. 1a and Fig. 1b we reported the intensity-weighted size distribution of GO and GO+PC hydrodynamic radius ( $R_H$ ) respectively at different sonication times (1, 5, 10 and 20 minutes). Distributions indicate that GO+PC sheets are systematically larger than native GO sheets. The increased value of the GO+PC  $R_H$  clearly manifests the presence of a huge amount of plasma proteins absorbed on the GO surfaces. Representative TEM images of a smooth and planar GO-sheet and of a rough GO+PC sheet with proteins absorbed are shown in insets of Fig.1a and Fig.1b respectively. In Fig.1c the mean value of  $R_H$  of GO and GO+PC at different sonication times is reported. Clearly there was a reduction of  $R_H$  with the increase of sonication time in both cases ranging from 660nm to 100nm and from 2260nm to 211nm for GO and GO+PC respectively. The  $\zeta$ -potential values of native GO sheets and GO+PC samples at different sonication times are reported in fig 1d. As

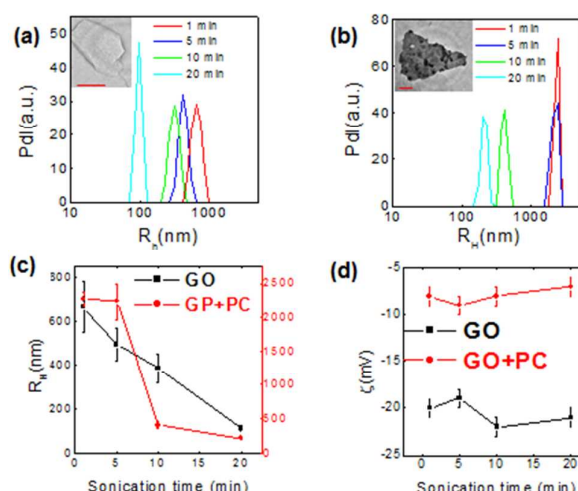


**Fig. 1** Intensity weighted radius distribution function (PdI) of GO (a) and GO+PC samples (b). TEM images of GO sheet and GO+PC sheet are shown in insets 1(a) and 1(b) scale bar is 150 nm. The mean value of hydrodynamic radius and its standard deviation, at different sonication time, are reported in fig.1(c) of both GO (black squares) and GO+PC (red dots) samples. In fig. 1(d) values of  $\zeta$ -potential at different sonication times are reported.

expected, GO samples show a higher  $\zeta$ -potential (about  $-20 \pm 1$  mV) than GO+PC<sup>19</sup> (about  $-8 \pm 1$  mV).

However the  $\zeta$ -potential values do not change significantly with the sonication time growing. This result suggests that in all the experimental conditions the plasma proteins forming the protein corona completely cover the GO flakes.

The morphology of GO with and without protein corona was investigated by AFM (Fig. 2a and Fig.2b). Sonication did not affect flakes morphology that remains planar and smooth in the GO case or rough in the GO+PC case. In Fig. 2c and 2d line profiles of GO flakes are plotted: GO sheet height is approximately 0,9nm (Fig. 2c), while height comprised between 5nm and 10nm were measured for GO+PC, indicating that serum protein were absorbed all over the surface after incubation<sup>20</sup>.

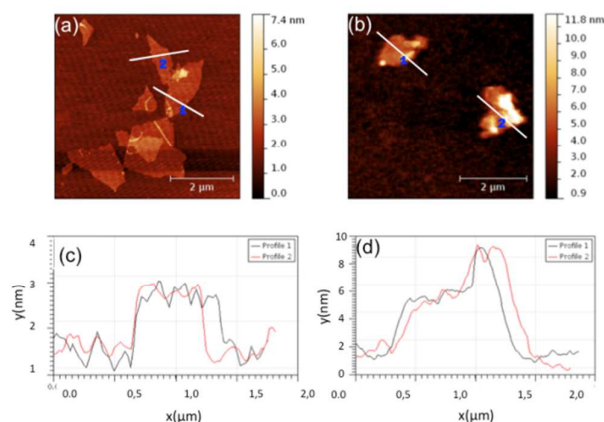


**Fig. 2** AFM images of GO (a) and GO+PC (b). In (c), (d) two line profiles show the height of both samples.

In Fig. 3a a photograph of RBCs samples after 3h exposure to GO (first row) and GO+PC (second row) is reported. The incubation of GO samples with RBCs revealed a very high haemolytic activity of the GO flakes, visible from the red colour due to the breaking of RBCs membrane and the consequent haemoglobin release. This effect appears to be strongly reduced for GO+PC showing that the presence of protein corona limits the haemolytic activity of GO on RBCs for every flake size considered. In Fig.3b the UV-VIS spectra of GO samples at different sonication times are reported. The absorbance increased with sonication time, reaching the maximum value with the negative control sample. The

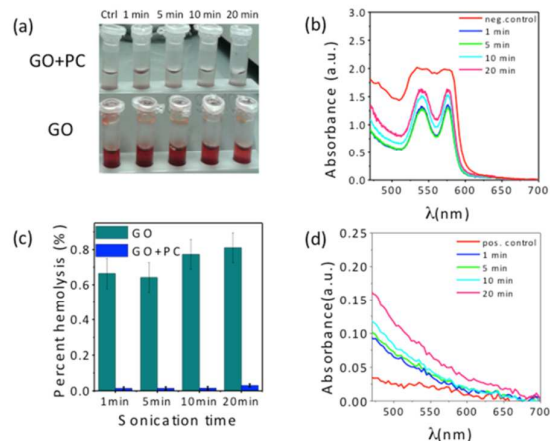


**Fig. 3** (a) Photograph of RBCs samples after 3h exposure to GO (first row) and GO+PC (second row) at different sonication times (1,5,10,20 minutes). (b) UV-VIS spectra of GO samples at different sonication time. (c) Percentage of haemolysis for both GO and GO+PC samples, calculated with eq.(6) (d) UV-Vis spectra of GO+PC samples at different sonication time.

variation of absorbance was from 0,9 (1 minute of sonication) to 1,8 (negative control). Moreover the spectra showed the typical features of heme absorption spectrum with two maxima at 540nm and 580nm, demonstrating that the haemoglobin in the RBCs was released in the supernatant after incubation with GO. In Fig. 3d the UV-Vis spectra of GO+PC samples at different sonication times are reported; absorbance

was lower than that of native GO samples, due to the lower concentration of free haemoglobin in the supernatants. Moreover the features of heme absorption were not present and no maxima were visible at 540 nm and 580 nm. In this case a little variation of absorbance of GO+PC samples, from 0,05 (positive control) to 0,15 (20 minutes sonication) was observed with increasing sonication time. In fig.3(c) a histogram indicating the percentage of haemolysis for both GO and GO+PC samples, calculated by Eq.1, was reported. Clearly there was an increase of haemolysis percentage as regards GO samples, from approximately 60% to 80%, linked to the GO flakes size reduction. Whereas GO+PC samples had significantly lower values of haemolysis from around 1 to 4% also linked to the GO-PC flakes size reduction.

In Fig.4 three representative confocal images of erythrocytes (a), erythrocytes after interaction with GO+PC (b) and after interaction with GO (c) are shown. The haemolytic activity of GO is clearly visible from the loss of the typical RBCs rounded shape. In the samples (b) and (c) fluorescent GO-PC and GO

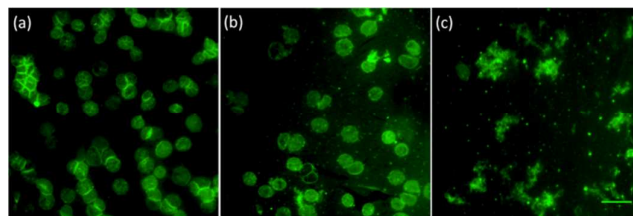


**Fig.4** Representative confocal images of erythrocytes (a), erythrocytes after interaction with GO+PC (b) and after interaction with GO (c).

flakes can be also observed.

## Conclusions

In conclusion, since GO flakes and injectable GO-related particles of different size could be used for biomedical applications<sup>1,2</sup>, in this paper we evaluated the GO and GO+PC biocompatibility with the red blood cells. We found that GO flakes have a very strong haemolytic activity increasing with the GO flakes size reduction. This activity was almost absent when the plasma protein corona was absorbed on the GO flakes surfaces. This phenomenon should be ascribed to the complex structural differences between GO+PC and GO such as surface charge, ROS production and absence of extremely sharp edges of graphene nanowalls. Similar haemolytic activity reduction has been recently observed on GO flakes coated by chitosan and amine, demonstrating that particle size, particulate state, oxygen content and surface charge of graphene have a strong impact on biological/toxicological effects on red blood cells. Finally we want to point out that our results highlight the fundamental and general role played by the plasma protein corona on the nano and micro GO flakes toxicity. Conversely, experiments describing a direct interaction between graphene-related particles and cells are not able to correctly determine the particles uptake and toxicity.

## Notes and references

- 1 H. Bao, Y. Pan and L. Li, *Nano LIFE*, 2012, **2**, 1230001-1230016.
- 2 H. Shen, L. Zhang, M. Liu and Z. Zhang, *Theranostics*, 2012, **2**, 283-294.
- 3 O. Akhavan, E. Ghaderi and A. Akhavan, *Biomaterials*, 2012, **33**, 8017-8025.
- 4 Y. Chang, S. T. Yang, J. H. Liu, E. Dong, Y. Wang, A. Cao, Y. Liu and H. Wang, *Toxicol. Lett.*, 2011, **200**, 201-210.
- 5 Y. Zhang, T. R. Nayak, H. Hong and W. Cai, *Nanoscale*, 2012, **4**, 3833-3842.
- 6 K. P. Loh, Q. Bao, G. Eda, and M. Chhowalla, *Nat. Chem.*, 2010, **2**, 1015-1024.
- 7 K.H. Liao, Y.S. Lin, C.W. MacOsco and C.L. Haynes, *ACS Appl. Mater. Interfaces*, 2011, **3**, 2607-2615.
- 8 O. Akhavan and E. Ghaderi, *ACS Nano*, 2010, **4** 5731e6.
- 9 W. Hu, C. Peng, M. Lv, X. Li, Y. Zhang, N. Chen, C. Fan and Q. Huang, *ACS Nano*, 2011, **5**, 3693-3700.
- 10 Y. Zhang, S.F. Ali, E. Dervishi, Y. Xu, Z. Li, D. Casciano et al., *ACS Nano*, 2010, **4**, 3181-3186.
- 11 M. Guo, M. Li, X. Liu, M. Zhao, D. Li, D. Geng, X. Sun and H. Gu, *J. Mater. Sci.: Mater. Med.*, 2013, **24**, 2741-2748.
- 12 S. K. Singh, M. K. Singh, P. P. Kulkarni, V. K. Sonkar, J. J. A. Gracio and D. Dash, *ACS Nano*, 2012, **6**, 2731-2740.
- 13 G. Caracciolo, F. Cardarelli, D. Pozzi, F. Salomone, G. Maccari, G. Bardi, A. L. Capriotti, C. Cavaliere, M. Papi and A. Laganà, *ACS Appl. Mater. Interfaces*, 2013, **5**, 13171-13179.
- 14 Zhang, J. Yin, C. Peng, W. Hu, Z. Zhu, W. Li, C. Fan and Q. Huang, *Carbon*, 2011, **49**, 986-995.
- 15 Y. Zhu, W. Li, Q. Li, Y. Li, Y. Li, X. Zhang, Q. Huang, *Carbon*, 2009, **47**, 1351-1358.
- 16 J. R. Hunter, *Zeta Potential in Colloid Science: Principles and Application Academic*, London, 1981.
- 17 M. Chiarpotto, G. Ciasca, M. Vassalli, C. Rossi, G. Campi, A. Ricci, B. Bocca, A. Pino, A. Alimonti, P. De Sole and, M. Papi, *Appl. Phys. Lett.*, 2013, 103, art. no. 083701.
- 18 V. Palmieri, D. Lucchetti, I. Gatto, A. Maiorana, M. Marcantoni, G. Maulucci, M. Papi, R. Pola, M. De Spirito and A. Sgambato, *J. Nanopart. Res.*, 2014, **16**, 1-8.
- 19 E. Casals, T. Pfaller, A. Duschl, G. J. Oostingh and V. Puntès, *ACS Nano*, 2010, **4**, 3623-3632.
- 20 S. Li, J. J. Mulloor, L. Wang, Y. Ji, C. J. Mulloor, M. Micic, J. Orbulescu, and Roger M. Leblanc, *ACS Appl. Mater. Interfaces*, 2014, **6**, 5704-5712.